A Fault Diagnosis Method for Power Systems Based on Temporal Tissue-like P Systems

Kequan Zhou, Tao Wang, Xiaotian Chen, and Quanlin Leng

Abstract—To quickly and accurately identify faulty components based on the alarm information is critical for the fault diagnosis of power grids. To address this challenge, this paper proposes a novel fault diagnosis method based on temporal tissue-like P system (TTPS). In the proposed method, suspected faulty components are identified first via a network topology analysis method. An TTPS-based fault diagnosis model is then built for each suspected faulty component to perform fault reasoning, so as to accurately detect the faulty components. To take full advantage of the action signals and temporal information of protection devices, TTPS and its forward temporal reasoning algorithm are proposed. TTPS can synchronously model the action and temporal logics of protection devices in an intuitive and graphical way, while the reasoning algorithm can process the fault alarm information in parallel. To demonstrate the effectiveness and superiority of the proposed method, simulations are carried out on the IEEE 14-bus and 118-bus systems, while the results are compared to other two widely adopted methods.

Index Terms—Alarm signal, fault diagnosis, membrane computing, power system, tissue-like P system.

I. INTRODUCTION

Fast and accurate fault diagnosis is of great importance for rapid power supply restoration after power outages [1]–[2]. However, with the gradual expansion of power system scales and the increasing complexity of their physical structures, new requirements are needed for fault diagnosis speed and accuracy after failure occurrence. So far, various fault diagnosis methods for power systems have been proposed, such as expert systems [3], Petri nets [4]–[8] and artificial neural networks [9]–[12].

Fault diagnosis methods based on expert systems are widely used in practical engineering. However, the construction of expert system-based diagnosis models are limited by the scale and protection configuration of the target power systems. Besides, their knowledge bases are difficult to maintain and the inference speed of models is usually slow. Conversely, Petri net-based models have the advantages of simple knowledge base structures and high computational efficiency. Nevertheless, when dealing with complex power systems, the models are complicated and have correlation matrices with high dimensions. Artificial neural networks (ANNs) have good robustness and strong learning ability, but their learning algorithms converge slowly. In addition, ANN-based models need to be retrained when grid structures change, so that they are less capable of adapting to the topology changes of power systems. Moreover, the diagnostic results of ANN-based models have poor interpretability. Therefore, fault diagnosis methods adapted to the development of power systems need to be continuously explored.

Membrane computing is a hot branch of natural computing, which aims at abstracting computing models from the structures and functioning of living cells, as well as from the collaboration ways of cells in tissues and organs [13]–[14]. It is becoming a research hotspot involving computer science, mathematics and biology. The computational models of membrane computing are called P systems, which have many outstanding advantages over traditional computational models. The theoretical computational efficiency of P systems can be higher than that of current electronic computers. In general, P systems can be classified into three types, namely, cell-like P system [15]–[16], neural-like P system [17]–[20] and tissue-like P system (TPS) [21]–[23].

Among the three types, TPS is a membrane computational model inspired by diverse individuals (e.g., cells, bacteria, social insects, etc.) exchanging information or chemical elements with each other in a specific environment. TPS has the advantages of being distributed, parallel, nondeterministic and extendibility to solve computationally difficult problems [21]. In recent years, many variants of TPS have been proposed based on biological facts, mathematical biological cells, computer science theory or application requirements. Reference [22] introduces evolutional symport/antiport rules into TPS, which are a class of distributed parallel

computing models inspired by the cell intercommunication in tissues. TPS with evolutional symport/antiport rules can be divided into two kinds: 1) symport/antiport rules are used to realize the communication between two given regions [30]; and 2) symport/antiport rules are controlled by the state of the region channel [31], [32]. Inspired by the biological balance mechanism, reference [29] introduces multiset rewriting rules into TPS and presents a homeostasis tissue-like P system, which can effectively solve NP-complete problems.

Meanwhile, many variants of TPS have been used in practical applications. For example, reference [32] proposes a new hybrid heuristic algorithm, which can better break through the limitations of the original single metaheuristic method to solve work-shop scheduling problems. A massively parallel algorithm for segmentation of digital images is developed to solve a region-based segmentation problem for digital images in [34]. To help doctors achieve detailed lesion identification, reference [35] explores a method for unsupervised and parallel segmentation of accurate segmentation of choroidal neovascularization in the optical coherence tomography. In [36], a fuzzy tissue-like P system (FTPS) is proposed to diagnose faults in power systems, which has the ability to deal with the uncertain fault messages and demonstrates the potential of TPS in the field of fault diagnosis. However, the disadvantages of the TPS-based model are also exposed. The object value of the output cell is represented by trapezoidal fuzzy numbers, which increases the subjectivity of the diagnosis method, whereas the TPS-based diagnosis model cannot use the temporal information in the alarm signals to deal with false and missed alarms.

In fact, the action information of protection devices collected by the SCADA system usually has uncertainty caused by misreported or missed information as well as missed or failed operation of protection devices. Such uncertainty may lead to a reduction in the accuracy of fault diagnosis. However, with the large-scale application of global positioning system (GPS) clock in power systems, a synchronous timestamp can be marked for each alarm message by the sequence of event (SOE) system. Therefore, the temporal order information can be used to correct the redundant errors by using the temporal order information consistency constraint relationship to filter out wrong alarm messages. Thus, more reliable alarm messages can be obtained after information error correction, which can overcome the uncertainty caused by maloperation and misrepresentation. In [37], a temporal abductive reasoning method is developed for power system fault diagnosis, in which the temporal constraint network is applied to describe the temporal constraints between events. To better evaluate the operating status of protective relays and circuit breakers, reference [38] presents a novel analytical model employing the temporal information of alarm messages. Although the existing work has used the temporal information, the interpretability and comprehensibility as well as the redundancy correction ability need to be further improved.

To address the aforementioned issues, this paper proposes a novel fault diagnosis method for power systems based on temporal tissue-like P systems (TTPSs). First, suspected faulty components are determined via the network topology analysis method, and based on the topology structure of the target power transmission network and the action logic of its protection devices, a diagnosis model based on TTPS is then built for each suspected fault components. The action order information of protection devices is subsequently employed to obtain the initial configuration vector of the diagnosis model, which is then modified with the consistency constraint of temporal characteristics. Finally, the forward temporal reasoning algorithm of each model is executed in a parallel manner to obtain the diagnosis results. The proposed TTPS not only has the advantages of traditional TPS, but also can fully utilize the temporal characteristics of fault alarm signals to deal with incomplete and uncertain messages from the SCADA system. The main contributions of this paper are described as follows:

1) To effectively deal with the uncertainty of fault information, a TTPS and its forward temporal reasoning algorithm are proposed. The proposed TTPS enables the forward reasoning and temporal information inference to work simultaneously. Simulations show that the consistency constraints of the temporal characteristics among different kinds of protection devices can well handle the uncertainty of alarm signals.

2) To improve the interpretability of the diagnosis models as well as reduce their complexity, an innovative virtual cells (VCs) and tissue fluid environment is introduced into TTPS. Based on this, four types of connection relations to describe the action sequence and logic of different protection devices are proposed. The highly visual modeling capability provides a more convenient way to understand the fault diagnosis process of power systems. Besides, presenting the temporal information in a graphical modeling way can also enhance the interpretability of the fault evolution process.

3) To improve the diagnostic accuracy, a novel fault diagnosis method based on TTPS and its forward temporal reasoning algorithm is proposed. Simulations show that the proposed diagnosis method not only has good fault tolerance, but also can describe the evolution of faults in a visual way with the graphical modeling process.

II. TEMPORAL REASONING OF ALARM MESSAGES

When a fault occurs in the power system, a large number of alarm signals with rich timing characteristics are transmitted to the dispatch center. The temporal

information of the alarm signals can be employed to reason out the fault evolution process, analyze fault causes as well as derive reasonable action behaviors of protective relays and circuit breakers. To be able to use the characteristics reasonably and adequately, a new variant of TPS, called the temporal tissue-like P system (TTPS), is proposed to improve the accuracy and fault tolerance of diagnosis results.

A. Temporal Constraints and Reasoning Operations

In [39], the time-point and time-distance constraints are proposed, which are defined as follows:

1) $[t_i^-, t_i^+]$ is the time-point constraint, where i is a time point; $T(i)$ represents that the event i occurs in $[t_i^-, t_i^+]$; whereas t_i^- and t_i^+ are the lower and upper bounds of $T(t)$, respectively.

2) $D(i,j) = [\Delta t_{ij}^-, \Delta t_{ij}^+]$ represents the time-distance constraint between the event i and event j, where Δt_{ij}^- and Δt_{ij}^+ are the lower and upper bounds of $D(i,j)$, respectively.

Since the two time constraints are defined by intervals, the temporal reasoning operations can also be defined by interval calculation rules as follows:

1) Forward reasoning: the time-point constraint of the event j can be inferred from $T(i)$ and $D(i,j)$; while $T(j)$ can be obtained as:

$$T(j) = T(i) + D(i,j) = [t_i^- + \Delta t_{ij}^-, t_i^+ + \Delta t_{ij}^+] \quad (1)$$

2) Backward reasoning: the time-point constraint of event i can be inferred from $T(j)$ and $D(i,j)$; while $T(i)$ can be obtained as:

$$T(i) = T(j) - D(i,j) = [t_j^- - \Delta t_{ij}^+, t_j^+ - \Delta t_{ij}^-] \quad (2)$$

B. Consistency Constraint of Temporal Characteristics

The time-distance calculations serve as the foundation of fault reasoning and diagnosis based on temporal information. Therefore, the consistency constraint of temporal characteristics can be used to determine whether protective relays or circuit breakers are maloperation, as well as identify uncertain situations such as misinformation.

In [40], the consistency constraint of temporal characteristics is defined as:

$$(T(i) + D(i,j)) \cap T(j) \neq \varnothing \quad (3)$$

Equation (3) represents that if the event j occurs at $T(j)$, $T(j)$ needs to satisfy the consistency constraint of temporal characteristics, i.e., $T(j) \subseteq (T(i) + D(i,j))$. If the event j satisfies the consistency constraint of temporal characteristics, the event j should complete within the time-point constraint $T(j)$; otherwise, the corresponding alarm signals are inaccurate alarm information.

III. TEMPORAL TISSUE-LIKE P SYSTEM

To make full use of the temporal information of alarm signals received from the SCADA systems, TTPS is proposed by introducing temporal elements on the connection channels of TPS, in which each cell node exchanges information. This section first gives the definition of the TTPS, and then explains in detail its initial configuration vectors, connection matrices, fault node vectors and the four kinds of correlations in the TTPS-based model.

A. TTPS

Definition 1: An TTPS of degree $m \geqslant 1$ is a tuple, i.e.:

$$\Pi = (O, \sigma_1, \cdots, \sigma_m, E, T, D, syn, i_0)$$

where

1) O is a non-empty alphabet whose element is called object;

2) $\sigma_i = (w_{i0}, R_{i1})$ or $\sigma_i = (w_{i0}, R_{i2})$, $1 \leqslant i \leqslant m$, is the i th tissue cell; and m is the number of tissue cells. The TTPS-based fault diagnosis model includes two types of tissue cells, namely, real cells and virtual cells (VC), whose forms are $\sigma_i = (w_{i0}, R_{i1})$ and $\sigma_i = (w_{i0}, R_{i2})$, respectively, where: ① w_{i0} denotes the initial object value on the alphabet O; ② $R_{i1} = (i, x/\lambda, j)$ is the transport rule of real cells, where x is the object in the cell i; λ is the object in the cell j and is an empty string. The object x in the cell i will be passed to the empty string λ in the cell j after the rule is executed; ③ $R_{i2} = (E, e/\lambda, VC)$ is the transport rule of VC, indicating main protection rejection or circuit breaker rejection; e is the object in the tissue fluid environment E; and λ is the object in VC. The object e in the tissue fluid environment E will be passed to the empty string λ in VC after the rule is executed.

3) $E = \{e_1, \cdots, e_n\}$ is the liquid environment of tissue cells (called tissue fluid environment), where $e_i \in O (1 \leqslant i \leqslant n)$ indicates the objects in E; and n is the number of the objects. If there is no direct channel for exchanging information between two tissue cells, then the environment can be used as an indirect channel to exchange messages. Consequently, when a real tissue cell does not satisfy the transport rule R_{i1}, it will perform the transport rule $(i, x/\lambda, E)$, where x is the object in the cell; λ is the object in E. The object x in the cell i will be passed to the empty string λ in E after the rule is executed;

4) $T = \{T(t_{\sigma i}) | \sigma_i \in \sigma\}$ is the time-point constraint of tissue cells, where $T(t_{\sigma i}) = [t_i^-, t_i^+]$ represents the time-point occurrence of the cell σ_i in the interval $[\Delta t_{ij}^-, \Delta t_{ij}^+]$;

5) $D = \left\{ D\left(\sigma_i, \sigma_j\right) \middle| \sigma_i, \sigma_j \in \sigma \right\}$ is the time-distance constraint of tissue cells, where $D\left(\sigma_i, \sigma_j\right) = \left[\Delta t_{ij}^-, \Delta t_{ij}^+\right]$ represents the time-distance between the occurrence of the cells σ_i and σ_j in the interval $\left[\Delta t_{ij}^-, \Delta t_{ij}^+\right]$;

6) $syn \subseteq \{1, \cdots, m\} \times \{1, \cdots, m\}$ denotes the connection channel between tissues cells in Π, where $i \neq j$ for all $(i, j) \in syn (1 \leqslant i, j \leqslant m)$;

7) $i_0 \in \{1, \cdots, n\}$ indicates the output cell set. It is worth noting that an output cell is marked as a suspected faulty component.

Definition 2: The initial configuration vector is $\boldsymbol{W}_0 = (w_{10}, \cdots, w_{m0})^{\mathrm{T}}$, where $w_{i0} (1 \leqslant i \leqslant m)$ equals to 0 or 1, representing the initial object in a tissue cell. If $w_{i0} = 1$, the protection device associated with σ_i has acted; otherwise, the protection device has not acted.

Since there are false alarm signals and maloperation of protection devices, when the action alarm signal of a protective relay is received without action information of corresponding circuit breakers, it is considered in this paper as a false alarm of the protective relay or the rejection of the corresponding circuit breaker. At the same time, the action signal value of the protective relay in $\boldsymbol{W}_0$ is set to 0. Likewise, when the action alarm signal of a circuit breaker is received without the action information of corresponding protective relay, it is considered as a false alarm of the circuit breaker or the false operation of the circuit breaker. At the same time, the action signal value of the circuit breaker in $\boldsymbol{W}_0$ is set to 0.

Definition 3: To better characterize the communication rules and causality of individual tissue cells, this paper introduces the connection matrix as follows:

$$C = (c_{ij})_{m \times m}, c_{ij} = \begin{cases} 1, & (i, j) \in syn \\ 0, & \text{other situations.} \end{cases} \quad (4)$$

where $\boldsymbol{C} = (c_{ij})_{m \times m}$ is a connection matrix. If there is a connection channel from σ_i to σ_j, then $c_{ij} = 1$; otherwise, $c_{ij} = 0$.

Definition 4: The fault node vector $\boldsymbol{S} = (s_1, \cdots, s_m)^{\mathrm{T}}$ of TTPS is given as:

$$s_i = \begin{cases} 1, & \text{when } \sigma_i \text{ is a suspected faulty} \\ & \text{component or a virtual cell;} \\ 0, & \text{other situations.} \end{cases} \quad (5)$$

where s_i represents the elements of the fault node vector. If σ_i is a VC or indicates a suspected faulty component, then $s_i = 1$; otherwise, $s_i = 0$.

Definition 5: Four types of connection relations of TTPS are shown in Fig. 1, and described as follows:

1) The faulty equipment corresponding to cell σ_i triggers the protection action corresponding to cell σ_j, as shown in Fig. 1(a).

2) The action of protections corresponding to cell σ_i triggers the circuit breaker action corresponding to cell σ_j, as shown in Fig. 1(b).

3) The rejection of the circuit breaker corresponding to cell σ_i triggers the action of protections corresponding to cell σ_j, as shown in Fig. 1(c), where a VC represents the rejection of a circuit breaker.

4) The rejection of the primary protection corresponding to cell σ_i triggers the action of the nearby backup protections corresponding to cell σ_j, as shown in Fig. 1(d), where a VC represents a main protection rejection.
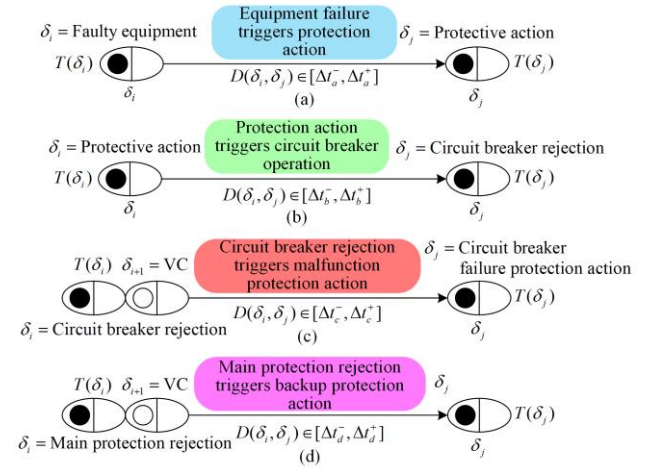

Fig. 1. Four types of correlations in TTPS.

In TTPS, the connection channels with different association relations have different time intervals, and the corresponding time distance constraints include $[\Delta t_a^-, \Delta t_a^+] \in [10, 40]$ ms, $[\Delta t_b^-, \Delta t_b^+] \in [40, 60]$ ms, $[\Delta t_c^-, \Delta t_c^+] \in [1900, 2100]$ ms, and $[\Delta t_d^-, \Delta t_d^+] \in [190, 240]$ ms, where $[\Delta t_a^-, \Delta t_a^+]$, $[\Delta t_c^-, \Delta t_c^+]$ and $[\Delta t_d^-, \Delta t_d^+]$ represent the time distance constraints between the moment of a line fault and the action moment of a main protection, first backup protection and second backup protection, respectively. $[\Delta t_b^-, \Delta t_b^+]$ denotes the time distance constraints between the action moment of a protective relay and its corresponding circuit breaker.

B. Forward Temporal Reasoning Algorithm

To enable the proposed TTPS to infer and process fault information in a parallel manner, this paper devises a forward temporal reasoning algorithm, as shown in Algorithm 1. To make the algorithm more intuitive, vectors, matrices and operators that will be used later are introduced here.

Algorithm 1 Forward temporal reasoning algorithm of TTPS

Input: *syn*, SCADA data and *S*

Step 1: The action information of protection devices received form the SCADA system is used to construct W_0 ;

Step 2: The connection relation syn in the TTPS-based fault diagnosis model is used to construct *C*;

Step 3: **if** alarm signal does not satisfy the consistency constraint of temporal characteristics, then correct W_0 and the algorithm jumps to Step 4;

Step 4: **else if** the algorithm jumps to Step 4 without the correction of initial configuration vector ;

Step 5: **end if**

Step 6) Calculate the transfer vector W_1 via $W_1 = W_0 \otimes C$;

Step 7: Calculate the judgment vector W_{end} via $W_{end} = W_1 \wedge S$;

Step 8: **if** $W_1 = 1$, **then** output judgement vector;

Step 9: **else if** the algorithm jumps to (11);

Step 10: **end if**

Step 11: $i = 2$;

Step 12: while $w_{1i} = 1$,**do**;

Step 13: Calculate W_i via $W_i = W_{i-1} \otimes C$;

Step 14: $i = i + 1$;

Step 15: **end while**

Step 16: define w_{1i} as the element W_1 of the judgment vector W_{end} .

Output: the output cell σ_{i0} in W_{end}

1) $W_0 = (w_{10}, \cdots, w_{m0})^T$ is the initial configuration vector of tissue cells (i.e., the statuses of protection devices and circuit breakers), where $w_{i0}(1 \leq i \leq m)$ equals to 0 or 1 and represents the initial value of the i th tissue cell. If the protection device associated with σ_i has acted, $w_{i0} = 1$; otherwise, $w_{i0} = 0$;

2) $C = (c_{ij})_{m \times m}$ is the connection matrix, which represents the connection channel from σ_i to σ_j . If there is a connection channel from σ_i to σ_j , $c_{ij} = 1$; otherwise, $c_{ij} = 0$;

3) $W_1 = (w_{11}, \cdots, w_{m1})^T$ is the transfer vector of tissue cells, where $w_{j1}(1 \leq j \leq m)$ equals to 0 or 1. If $w_{i0} \wedge c_{ij} = 1$ $(1 \leq i \leq m, j = 1, \cdots, m)$, $w_{j1} = 1$; otherwise, $w_{j1} = 0$;

4) $S = (s_1, \cdots, s_m)^T$ is a fault node vector, where $s_i(1 \leq i \leq m)$ equals to 0 or 1, representing node distribution of failed components. If σ_i is a suspected faulty component or a VC, $s_i = 1$; otherwise $s_i = 0$;

5) $W_{end} = (w_1, \cdots, w_m)^T$ is a judgment vector of tissue cells, where $w_i(1 \leq i \leq m)$ equals to 0 or 1. If σ_i corresponds to a faulty component, $w_i = 1$; otherwise $w_i = 0$;

6) $W_1 = W_0 \otimes C = (w_{11}, \cdots, w_{m1})^T$, where $w_{i1} = (c_{i1} \wedge w_{11}) \vee \cdots \vee (c_{mi} \wedge w_{m1})(1 \leq i \leq m)$. For $\forall a, b$ equals to 0 or 1, it defines that $a \wedge b = \min\{a, b\}$ and $a \vee b = \max\{a, b\}$;

7) $W_{end} = W_1 \wedge S = (w_1, \cdots, w_m)^T$, where $w_i = w_{i1} \wedge s_i$, $i = 1, \cdots, m$.

Afterwards, to enable TTPS to calculate fault alarm information, its parallel reasoning algorithm is proposed in Algorithm 1.

IV. FAULT DIAGNOSIS METHOD BASED ON TTPS

This section proposes a fault diagnosis method for transmission networks based on TTPS, and the flowchart is shown in Fig. 2. Detailed steps of the proposed method are described as follows:
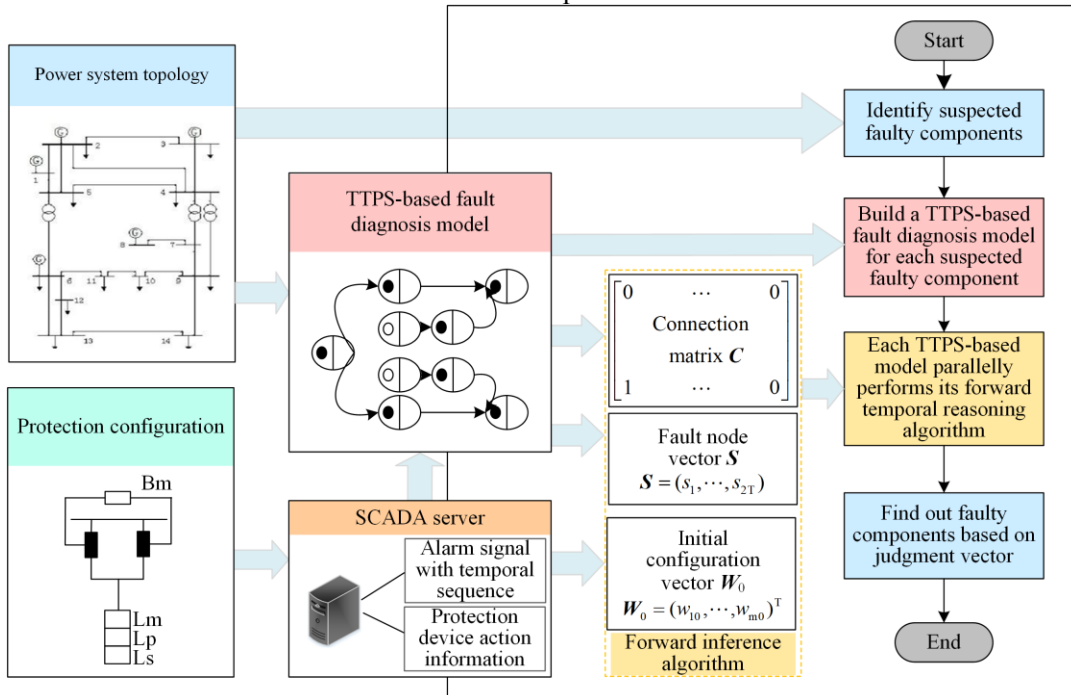

Fig. 2. Framework of fault diagnosis of power system based on TTPS.

Step 1: Identify suspected faulty components. Determine fault areas via the network topology analysis method [40], so as to find out suspected fault components;

Step 2: Build a TTPS-based fault diagnosis model for each suspected fault component based on the topology structure of the target power transmission network and the action logic of its protection devices;

Step 3: Each TTPS-based diagnosis model performs its forward temporal reasoning algorithm in a parallel manner to calculate the judgment vector of its output cell. Step 3 is described as follows:

1) Use the action messages of protection devices received from the SCADA system to construct initial configuration vector;

2) Construct connection matrix C via Step 2 for each TTPS-based fault diagnosis model;

3) Construct fault node vector according to the TTPS-based model for each suspicious fault component;

4) Each TTPS-based model performs its forward temporal reasoning algorithm in a parallel manner based on W_0, C and S;

5) Calculate judgment vector of the output cell via $W_{end} = W_1 \wedge S$.

Step 4: Output diagnosis results. Find out faulty components according to the object values of the judgment vector. If the element value of the judgment vector equals to 1, then its corresponding component is at fault; otherwise, it is not faulty.

To improve the intelligibility, a sketch map of the building process of a TTPS-based diagnosis model is shown in Fig. 3. In Fig. 3(a), a simple power transmission system is represented, which includes one line (i.e., L), two circuit breakers (i.e., CB1 and CB2), two main protections (i.e., MLR1 and MLR2), and two back up protections (i.e., BLR1 and BLR2). If a fault occurs on line L, then MLR1 and MLR2 will act to trip the circuit breakers CB1 and CB2. If MLR1 and MLR2 fail to act, then BLR1 and BLR2 will trip the circuit breakers CB1 and CB2.

The TTPS-based diagnosis model of the simple power

transmission system is shown in Fig. 3(b). It consists of nine tissue cells, which are associated with L, VC, MLR1, MLR2, BLR1, BLR2, CB1 and CB2, respectively. Line L corresponding to cell σ_1 is an output cell, and VC denotes the main protection fails to operate. In the TTPS-based model, the solid line directed arcs represent the causal relationship between protection devices, while the blue dashed lines denote the direction of Algorithm 1. Moreover, the time interval on the directed arc indicates that the association relationships of different connection channels have different time distance constraints.
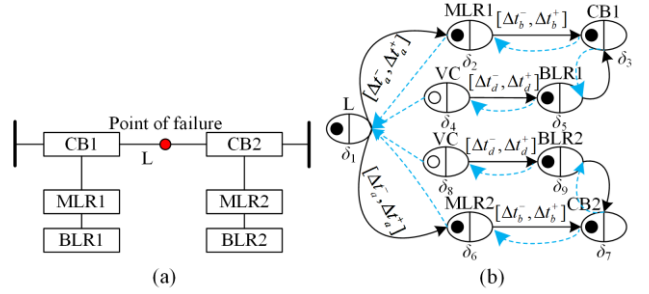

Fig. 3. A sketch map of the building process of a TTPS-based diagnosis model. (a) A simple transmission network. (b) Its TTPS-based fault diagnosis mode.

V. EXPERIMENTAL RESULTS AND ANALYSIS

The proposed method is applied to the IEEE 14-bus and 118-bus systems to demonstrate its effectiveness and superiority.

A. Case Study

1) IEEE 14-bus System

The topology of an IEEE 14-bus system is illustrated in Fig. 4. Six cases including different failure scenarios, such as single fault and multiple failures with maloperation and misinformation, are used to compare the proposed method with other two existing ones, i.e., the fuzzy reasoning spiking neural P system (FRSNPS) in [42] and the cause effect network (CEN) in [43]. The two methods are chosen because that they have been widely used for the fault diagnosis of power systems and have been verified to be superior.
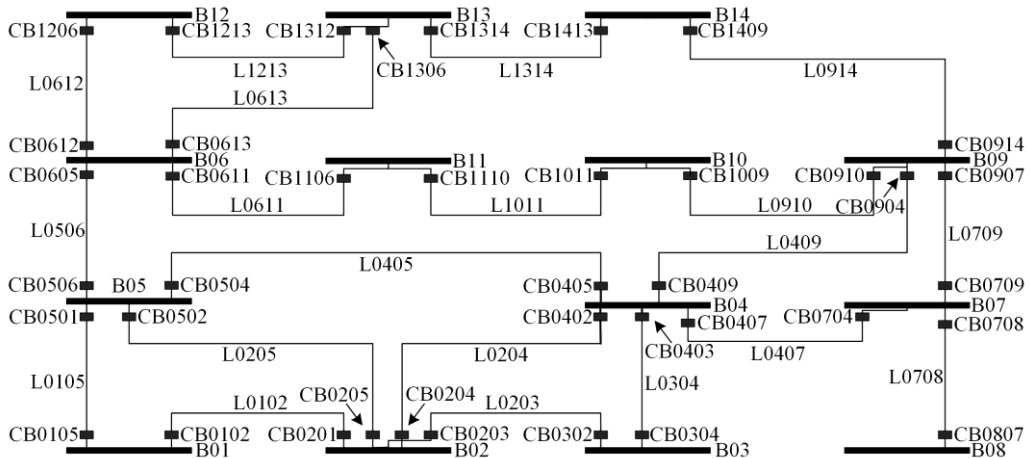

Fig. 4. IEEE 14-bus power system.

The diagnostic results are shown in Table I, where the information in the first column represents alarm signals received from the SCADA system. Specifically, "L" denotes a line; "B" denotes a bus; "CB" denotes a circuit breaker; "m" denotes the main protection of lines; "p" denotes the nearby backup protection of lines; and "s" denotes the remote backup protection of lines. For example, L1413s (1989) represents that the action signal of the remote backup protection of L1413 is received at 1989 ms. Moreover, the information in the fifth column of Table I represents the time-point constraint of fault moment. For instance, the information in the fifth column for case 1 represents that the line "L0708" is failed in time point constraint [-20, -10] ms. Besides, "MO", "RO", "EA", "MA" and "FT" in the sixth column are described at the bottom of Table I.

TABLE I
COMPARISONS OF DIAGNOSIS RESULTS BETWEEN THE PROPOSED METHOD AND TWO TYPICAL FAULT DIAGNOSIS METHODS FOR IEEE 14-BUS SYSTEM

No.	Action information of protection devices	Suspected faulty equipment	Actual faulty equipment	Time-point constraint (ms)	The proposed method		FRSNPS [41]	CEN [42]
					Information evaluation	Diagnosis results		
1	L0708m(0), L0807m(3), CB0708(48), CB0807(51)	L0708	L0708	[−20, −10]	Correct action	L0708	L0708	L0708
2	B13m(0), CB1312(48), CB1306(51), L1413m(48), L1413s(1989), CB1413(2044)	B13 L1213, L1314	B13	[−20, −10]	L1413m, MO CB1314, RO	B13	B13, L1314	B13 L1314
3	L1213s(0), L0613s(7), L1413s(9), CB1213(54), CB0613(58), CB1413(60)	B13, L0613, L1213, L1314	B13	[−2091, −1900]	B13m, RO	B13	B13	B13
4	L1314m(0), CB1314(48), L1413p(530), CB1413(545)	L1314	L1314	[−20, −10]	L1413m, RO L1413p, FT	L1314	L1314	L1314
5	L1314m(0), B13m(30), CB1314(48), CB1413(50), CB1312(81), CB1306(82)	L1314 B13	L1314 B13	[−20, −10] [10, 20]	Correct action	L1314 B13	L1314 B13	L1314 B13
6	B13m(0), CB1312(48), CB1306(51), L1314m(200), B07m(250), CB0708(301), L1413s(1989), CB1413(2041)	B13 B07 L1314	B13 B07	[−20, −10] [230, 240]	CB1314, RO L1314m, EA CB0709, MA CB0704, MA	B13 B07	B13 B07 L1314	B13 B07 L1314
7	B11m(0), L1011m(3), L1101m(5), CB1106(48), CB1110(52), CB1011(54), L0910m(101), L1009m(103), CB0910(153), CB1009(156)	B11 B10 L1011 L0910	B11 L1011 L0910	[−20, −10] [−17, −10] [80, 90]	B10m, EA	B11 L1011 L0910	B11 B10 L1011 L0910	B11 B10 L1011 L0910
8	B02m(0), CB0201(47), CB0205(49), CB0204(51), L1314m(518), CB1314(566), L1413p(702), CB1413(751), L1110s(2085), L0910s(2088), CB1110(2138), CB0910(2140)	B02 B10 L1011 L0910 L1314	B02 B10 L1314	[−20, −10] [80, 90] [495, 505]	B10m, RO L1314m, RO CB0203, MA	B02 B10 L1314	B02 B10 L1314	B02 B10 L1314
9	B02m(0), CB0201(47), CB0205(49), CB0204(51), CB0203(52), L0203m(55), B10m(102), L1011m(99), L1101m(101), CB1011(145), CB1009(148), B13m(250), CB1314(294)	B02 B10 B13 L0203 L1011	B02 B10 B13 L1011	[−20, −10] [80, 90] [230, 240] [77, 90]	L0203m, MO CB1312, MA CB1306, MA	B02 B10 B13 L1011	B02 B10 B13 L0203 L1011	B02 B10 B13 L1011
10	B11m(0), CB1106(47), CB1110(49), B02m(99), CB0201(147), CB0205(149), CB0204(151), CB0203(152), L1314m(250), CB1314(312), L1413p(438), CB1413(480), L0613m(562), L1306m(565), CB0613(605), B14m(607), CB1306(608)	B11 B02 B13 L1314 L0613	B11 B02 L1314 L0613	[-20, -10] [80, 90] [230, 240] [540, 550]	B13m, EA L1413m, RO	B11 B02 B13 L1314 L0613	B11 B02 B13 L1314 L0613	B11 B02 B13 L1314 L0613

Notes: "m" represents the main protective relay; "p" represents the nearby backup relay; "s" represents the remote backup relay; "RO" means that the protective device refuse to operate; "MO" represents the maloperation of protective device; "EA" represents the error alarm of protective device; "MA" represents the missing alarm of protective device; "FT" represents the alarm signal has a false timestamp.

It can be seen from Table I that cases 1, 3, 5 and 8 have complete and accurate fault information while cases 2–4, 6, 7, 9 and 10 are accompanied by rejection or maloperation or omission or misrepresentation of pro-

tection devices. Furthermore, cases 1–4 are the single fault while cases 5-10 are the multiple failures. For cases 1, 3, 4, 5 and 8, all the fault diagnostic results of TTPS, FRSNPS and CEN are correct. For case 2, both CEN and FRSNPS misdiagnose line L1314 as a faulty component because of the maloperation of L1413m, whereas TTPS accurately finds the faulty component by judging the consistency constraint of temporal characteristics of the protection devices. For cases 6, 7, 9 and 10, both CEN and FRSNPS fail to correctly find faulty components due to the incorrect key alarm signals, while TTPS can still find the correct faulty components. The TTPS-based fault diagnosis models for the suspected faulty components involved in cases 1−2 in Table I are shown in Figs. 5−9, and Fig. A1. Due to space limitation, the diagnostic models of the suspected faulty components involved in cases 3−10 are shown in Appendix A.
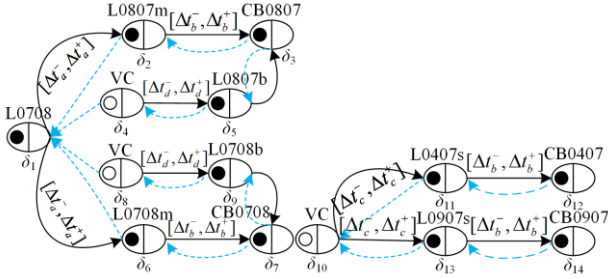

Fig. 5. TTPS-based fault diagnosis model of L0708.
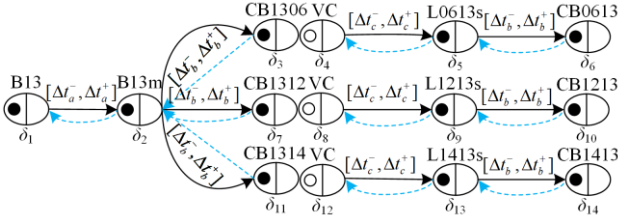

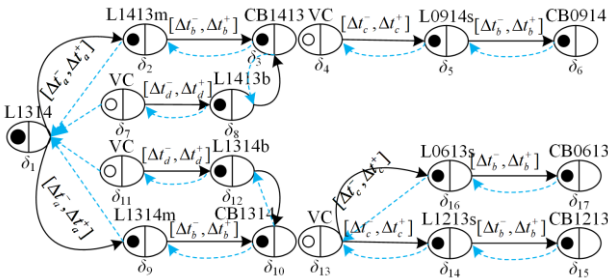Fig. 6. TTPS-based fault diagnosis model of B13.

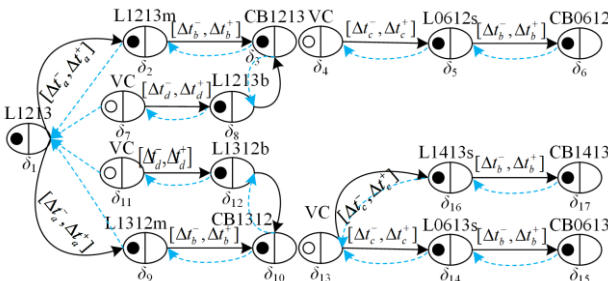Fig. 7. TTPS-based fault diagnosis model of L1314.

Fig. 8. TTPS-based fault diagnosis model of L1213.

The reasoning process of case 2 is given here as an example. Assuming a fault occurs at bus B13, and causes the main protective relay B13m to operate, circuit breakers CB1312 and CB1306 to trip, and CB1314 to reject, resulting in the nearby backup protective relay L1413 s to operate and the circuit breaker CB1413 to trip. The fault is also accompanied by the false operation of L1413 m and the rejection of circuit breaker CB1314. The received alarm sequence with time scale is shown in Table I.

The proposed TTPS fault diagnosis model for bus B13 is shown in Fig. 6, which consists of 14 tissue cells, i.e., $(\sigma_1,\cdots,\sigma_{14})$. Based on the TTPS-based fault diagnosis model of B13, a 14×14 connection matrix $\boldsymbol{C}$ is obtained as follows:

$$\boldsymbol{C} = \begin{pmatrix} 0 & 0 & 0 & \cdots & 0 & 0 & 0 & 0 \\ 1 & 0 & 0 & \cdots & 0 & 0 & 0 & 0 \\ 0 & 1 & 0 & \cdots & 0 & 0 & 0 & 0 \\ 0 & 0 & 0 & \cdots & 0 & 0 & 0 & 0 \\ 0 & 0 & 1 & \cdots & 0 & 0 & 0 & 0 \\ 0 & 0 & 0 & \cdots & 0 & 0 & 0 & 0 \\ \vdots & \vdots & \vdots & & \vdots & \vdots & \vdots & \vdots \\ 0 & 1 & 0 & \cdots & 0 & 0 & 0 & 0 \\ 0 & 0 & 0 & \cdots & 0 & 0 & 0 & 0 \\ 0 & 0 & 0 & \cdots & 0 & 1 & 0 & 0 \\ 0 & 0 & 0 & \cdots & 0 & 0 & 1 & 0 \end{pmatrix}$$

According to the action information of protection devices provided by the SCADA system, the initial configuration vector, i.e., $\boldsymbol{W}_0$, can be obtained as:

$$\boldsymbol{W}_0 = (0,1,1,0,0,0,1,0,0,0,0,0,1,1)^{\mathrm{T}}$$

Then, according to the distribution of suspected faulty components and virtual cells according to the TTPS-based fault diagnosis model, the fault node vector, i.e., $\boldsymbol{S}$, can be constructed as:

$$\boldsymbol{S} = (1,0,0,1,0,0,0,1,0,0,0,1,0,0)^{\mathrm{T}}$$

The forward temporal reasoning algorithm is performed to obtain the judgment vector of output cell of the diagnosis model, i.e., $\boldsymbol{W}_{\mathrm{end}}$, as:

$$\boldsymbol{W}_{\mathrm{end}} = (1,0,0,0,0,0,0,0,0,0,0,1,0,0)^{\mathrm{T}}$$

Consequently, bus B13 is determined as a faulty component. In addition, according to the judgment vector, it is found that CB1314 fails to operate. Likewise, it is found that lines L1213 and L1314 are not at fault. Table I shows that the main protection L1413m of line L1413 acts at 48 ms and the corresponding circuit breaker CB1413 trips at 2044 ms. According to the consistency constraint of temporal characteristics, there is $\Delta t \notin [40,60]$ ms. Thus, the time-distance constraint rule is not satisfied. Consequently, line L1413 is maloperation and its initial configuration vector needs

to be corrected. It can be seen that line L1314 will be misdiagnosed as a faulty component without the judgment of the consistency constraint of temporal characteristics.

The analysis process of fault evolution is described as follows. The time scale of the first alarm received is employed as the reference point. The actual fault evolution process is inferred by analyzing the timing sequence, i.e.: bus B13 fails during [−20, −10] ms; the main protection B13m operates at 0 ms and triggers CB1312 and CB1306 to operate at 48 ms and 51 ms, respectively; CB1314 fails to trip, while the operation of the remote backup protection L1413s at 1989 ms trips CB1413 at 2041 ms.

2) IEEE 118-Bus System

In this subsection, a complex IEEE 118-bus system is employed to further verify the efficiency of the proposed method. The system has 118 buses, 132 lines and 257 circuit breakers. The system is divided into 4 sub-networks (i.e., S1, S2, S3 and S4) via the weight network segmentation method in [44], as shown in Fig. 9. The lines, circuit breakers and protective relays are named based on the number of the buses. For example, the line connecting buses B05 and B08 is numbered as L0508, the corresponding circuit breaker on the side of B05 is numbered as CB0508 while the one on the opposite side is numbered as CB0805. Ten cases are considered for comparison between the proposed method, CEN and FRSNPS.
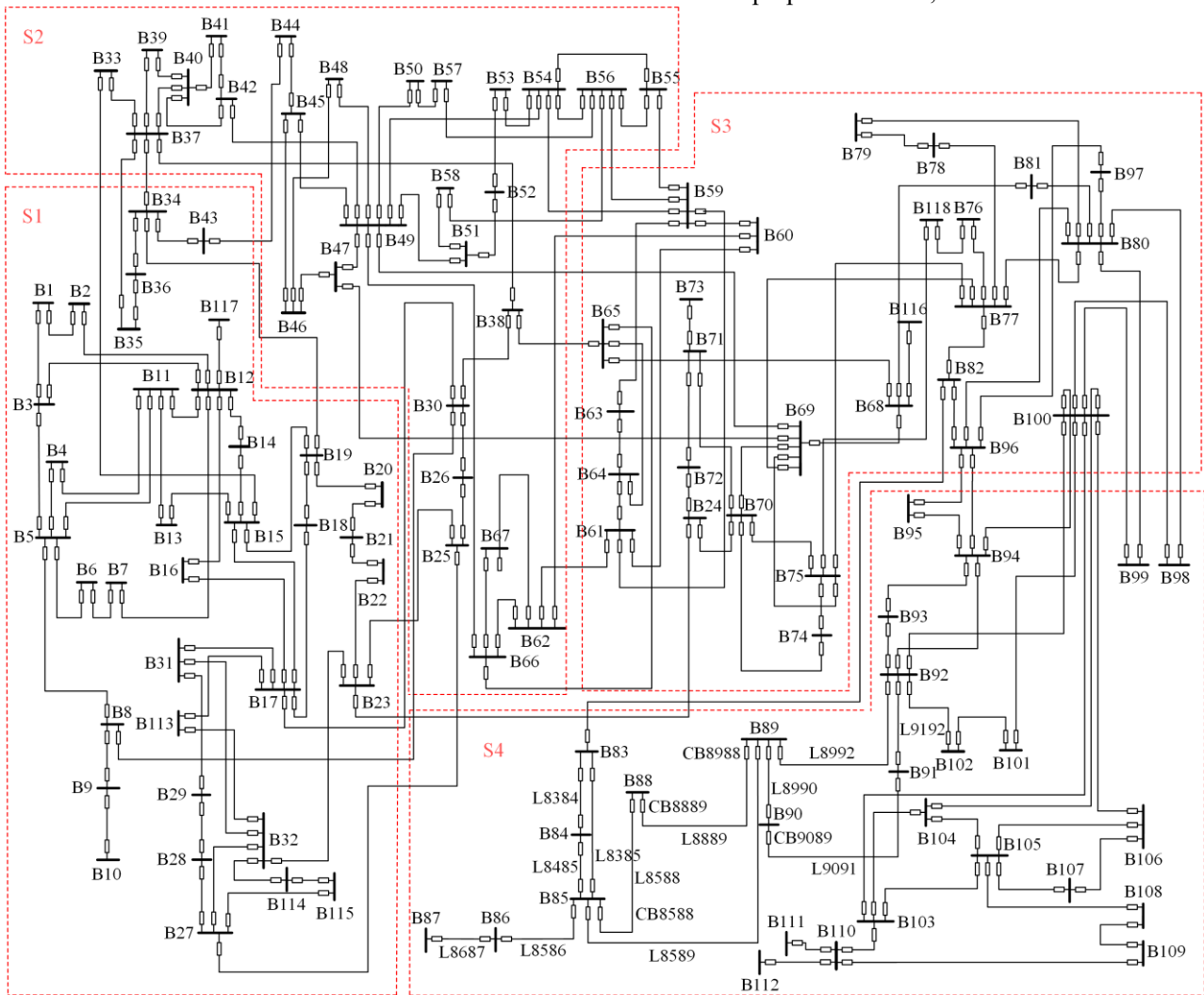

Fig. 9.   IEEE 118-bus power system.

The results are shown in Table II. As seen, cases 1, 2 and 5 have complete and accurate fault information while cases 2–4 and 6–10 are accompanied by rejection or maloperation or omission or misrepresentation of protection devices. Furthermore, case 1 is the single fault while cases 2–10 are the multiple failures. For cases 1, 2, 4–6 and 8, all the fault diagnostic results of TTPS, FRSNPS and CEN are correct. For cases 3 and 9, both CEN and FRSNPS misdiagnose lines L1819 and L0102 as faulty components because of the maloperation of L1819 m and L0102 m, while TTPS can still accurately find the faulty component by judging the consistency

constraint of the temporal characteristics of protection devices. For case 10, due to the omission of key alarm signals, both CEN and FRSNPS fail to correctly find the faulty components, while TTPS can correctly find the faulty components. Thus, it is evident that the proposed method can obtain satisfying results for a complex system with fault information errors.

TABLE II
COMPARISONS OF DIAGNOSIS RESULTS BETWEEN THE PROPOSED METHOD AND TWO TYPICAL FAULT DIAGNOSIS METHODS FOR IEEE 118-BUS SYSTEM

No.	Action information of protection devices	Suspected faulty equipment	Actual faulty equipment	Time-point constraint (ms)	The proposed method		FRSNPS [42]	CEN [43]
					Information evaluation	Diagnosis results		
1	B83m(0), CB8384(48), CB8385(50), CB8382(51)	B83	B83	[−20, −10]	Correct action	B83	B83	B83
2	L0508 m(0), L0805 m(2), CB0508(48), CB0805(50), L1216s(2019), L1716s(2021), CB1216(2069), CB1716(2072)	B16 L1216 L1617 L0508	B16 L0508	[10, 20] [−20, −10]	B16m, RO	B16 L0508	B16 L0508	B16 L0508
3	L3419 s(0), L1519 s(7), L1819 s(9), L2019 s(10), L2527 m(30), L2725 m(32), CB3419(48), CB1519(55), CB1819(57), CB2019(59), CB2527(88), CB2725(90), L1819m(93)	B19 L2527 L1934 L1519 L1819 L1920	B19 L2527	[−2090, −1900] [10, 20]	B19m, RO L1819m, MO	B19 L2527	B19 L1819 L2527	B19 L1819 L2527
4	L6267 m(0), CB6267(48), L8992m(30), L9289 m(32), CB8992(80), CB9289(82), L6762 p(530), CB6762(545)	L6267 L8992	L6267 L8992	[−20, −10] [10, 20]	L6762m, RO L6762p, FT	L6267 L8992	L6267 L8992	L6267 L8992
5	B53 m(0), B79 m(30), CB5352(48), CB5354(50), CB7978(79), CB7980(82), L7173 m(99), L7371 m(101), CB7173(149), CB7371(151)	B53 B79 L7173	B53 B79 L7173	[−18, −10] [10, 20] [80, 90]	Correct action	B53 B79 L7173	B53 B79 L7173	B53 B79 L7173
6	B38 m(0), B59 m(30), CB3830(48), CB3865(50), CB5961(79), CB5956(81), CB5954(83), CB5963(86), L2223m(250), L2322 m(252), CB2223(298), CB2322(301), L3738 s(1990), CB3738(2040)	B38 B59 L2223 L3738	B38 B59 L2223	[−20, −10] [10, 20] [230, 240]	CB3837, RO CB5960, MA CB5955, MA	B38 B59 L2223	B38 B59 L2223	B38 B59 L2223
7	B51 m(0), L5851m(3), L2931 m(30), L3129 m(33), CB5149(48), CB5851(50), L5158 m(57), CB2931(81), L3231p(1005), L3231 s(2019), L1731 s(2021), CB3231(2068), CB1731(2070)	B51 L5158 L2931 L3132 L1731	B51 L5158 L2931	[−18, −8] [−20, −10] [10, 20]	CB5158, MA CB5152, MA L5158m, FT CB3129, RO L3231p, EA	B51 L5158 L2931	B51 L5158 L2931 L3132	L5158 L2931 L3132
8	L4037 s(0), L3937 s(2), L3337 s(5), L3537 s(6), L3437 s(7), L3837 s(9), B67m(30), CB4037(48), CB3337(52), CB3537(54), CB3437(55), CB3837(57), CB6766(78), CB6762(81), B83 m(99), CB8384(147), CB8385(149), CB8382(151), L4549 m(249), L4945 m(251), CB4549(297), CB4945(299)	B37 B67 B83 L4549 L3740 L3739 L3337 L3537 L3437 L3738	B37 B67 B83 L4549	[−2040, −1950] [10, 20] [80, 90] [230, 240]	B37m, RO CB8384, MA CB3937, MA	B37 B67 B83 L4549	B37 B67 B83 L4549	B37 B67 B83 L4549
9	B22 m(0), L0805 m(30), CB2223(48), CB0508(78), CB0805(81), L0607 m(249), L0706 m(251), CB0706(298), L0301 m(504), L0103 m(506), CB0301(552), L0102 p(560), L0201 s(2495), CB0201(2542)	B22 L0508 L0607 L0103 L2122 L0102	B22 L0508 L0607 L0103	[−20, −10] [10, 20] [230, 240] [485, 495]	CB22221, RO L0508m, MA CB0607, MA CB0103, RO L0102p, MO	B22 L0508 L0607 L0103	B22 L0508 L0607 L0103 L0102	B22 L0508 L0607 L0103 L0102
10	B53 m(0), L5354 m(3), L5453 m(5), CB5354(49), CB5453(50), B55 m(250), CB5556(297), L5559 p(438), L5253 m(450), L5253 s(1989), CB5253(2037)	B53 B55 L5354 L5559 L5253	B53 B55 L5354 L5559	[−17, −10] [230, 240] [−20, −10] [234, 240]	L5253m, FT CB5352, RO CB5554, MA CB5559, MA L5559m, RO	B53 B55 L5354 L5559	B53 B55 L5354 L5559 L5253	B53 L5354 L5559 L5253

Notes: "m" represents the main protective relay; "p" represents the nearby backup relay; "s" represents the remote backup relay; "RO" means that the protective device refuse to operate; "MO" represents the maloperation of protective device; "EA" represents the error alarm of protective device; "MA" represents the missing alarm of protective device.

B. Accuracy Test

To verify the fault-tolerant ability and universality of the proposed method, the accuracy tests under different ratios of uncertain information are carried out. The ratio is defined as:

$$k = \frac{I_{\text{rand}}}{I_{\text{fault}}} \times 100\% \qquad (6)$$

where I_{rand} is the number of the uncertain fault alarm messages and I_{fault} is the number of fault alarm mes-

sages received from the SCADA system. The uncertain information is obtained by simulating the rejection and maloperation of protection devices as well as the information loss and distortion during the signal transmission process.

1) IEEE 14-bus System

The fault diagnosis accuracies of the three methods analyzed above based on the IEEE 14-bus system are tested and the comparison results are shown in Table III. To ensure the universality of the experimental results, each diagnosis accuracy in Table III is obtained based on the IEEE 14-bus system by testing 100 000 times. Table III shows that all the three methods can accurately diagnose the faults when the fault alarm messages are completely accurate (i.e., $k = 0\%$). When the ratios of uncertain information are low, such as $k = 1\%$ and $k = 2\%$, the diagnosis accuracies of the three methods are all high with negligible difference. However, when the ratio of uncertain information rises, the diagnosis accuracy of FRSNPS has the fastest decrease among the three methods. For example, when $k = 4\%$, the diagnosis accuracies of TTPS and CEN remain high (i.e., 0.9862 and 0.9818, respectively), whereas that of FRSNPSS is only 0.9666. When the ratio of uncertain information continues to rise, TTPS maintains the highest diagnostic accuracy, while FRSNPS has the lowest accuracy.

TABLE III
ACCURACY TESTS OF THREE METHODS FOR DIFFERENT K BASED ON IEEE 14-BUS SYSTEM

k	TTPS	FRSNPS	CEN [43]
0	1	1	1
1	0.9963	0.9917	0.9957
2	0.9922	0.9833	0.9907
3	0.9893	0.9750	0.9860
4	0.9862	0.9666	0.9818
5	0.9826	0.9582	0.9772
6	0.9786	0.9500	0.9723
7	0.9755	0.9417	0.9682
8	0.9723	0.9333	0.9636
9	0.9681	0.9248	0.9586
10	0.9620	0.9164	0.9534
20	0.9241	0.8329	0.9037
30	0.8902	0.7498	0.8545

2) IEEE 118-bus System

To further verify the effectiveness and superiority of the proposed method, the IEEE 118-bus system is employed to carried out the tests for different k. The test method is the same as that of the IEEE 14-bus system and the comparison results are shown in Table IV. Similar to previous tests, each diagnosis accuracy for different k is tested 100 000 times. From Table IV, it can be seen that, for such a complex power system, all the three methods can accurately diagnose the faults when the fault alarm messages are completely accurate (i.e., $k = 0\%$). When

the ratios of uncertain information are low (e.g., under $k = 3\%$), the diagnosis accuracies of the three methods are high. However, when the ratio of the uncertain information rises, the diagnosis accuracy of FRSNPS sees the fastest decrease while TTPS maintains the highest diagnosis accuracy. The accuracy change trends of the three methods are the same as those of the IEEE 14-bus system. Comparing Table III with Table IV, it is seen that, for the same method and uncertain information ratio, there is only a small difference between the data obtained from the systems. Therefore, the results verified that TTPS can effectively handle the imprecise and uncertain fault alarm messages to detect faulty components with high fault-tolerance for complex systems.

TABLE IV
ACCURACY TESTS OF THREE METHODS FOR DIFFERENT K BASED ON IEEE 118-BUS SYSTEM

k	TTPS	FRSNPS	CEN [43]
0	1	1	1
1	0.9969	0.9919	0.9959
2	0.9932	0.9838	0.9911
3	0.9904	0.9757	0.9871
4	0.9874	0.9676	0.9831
5	0.9842	0.9594	0.9786
6	0.9806	0.9513	0.9740
7	0.9775	0.9433	0.9700
8	0.9746	0.9352	0.9662
9	0.9709	0.9268	0.9618
10	0.9673	0.9188	0.9577
20	0.9333	0.8379	0.9143
30	0.8991	0.7565	0.8706

VI. CONCLUSIONS

In this paper, a novel TTPS-based fault diagnosis model is proposed for diagnosing faults in power systems. The proposed TTPS can not only reason out the time interval at the moment of fault occurrence, but also explain the whole evolution of fault. The proposed method has high diagnostic accuracy with good tolerance and interchangeability. Experiments based on the IEEE 14-bus and 118-bus systems demonstrate that the proposed method can effectively deal with single and complex faults with incorrect alarm signals. Future efforts will take account of the impact of meteorological factors on the uncertainty of fault alarm information, so as to further enhance its diagnosis accuracy and reliability.
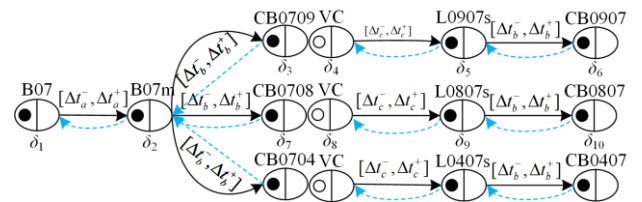
APPENDIX A

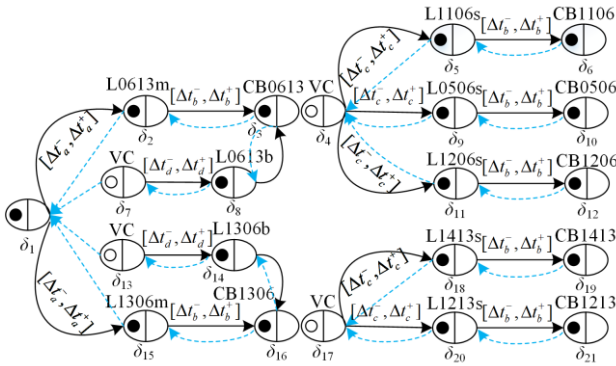
Fig. A1. TTPS-based fault diagnosis model of B07.

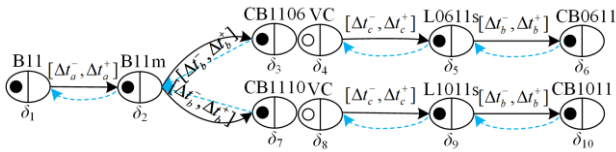Fig. A2. TTPS-based fault diagnosis model of L0613.

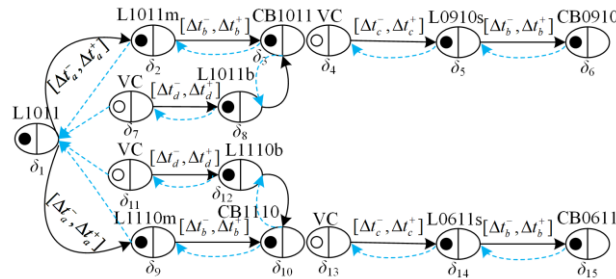Fig. A3. TTPS-based fault diagnosis model of B11.

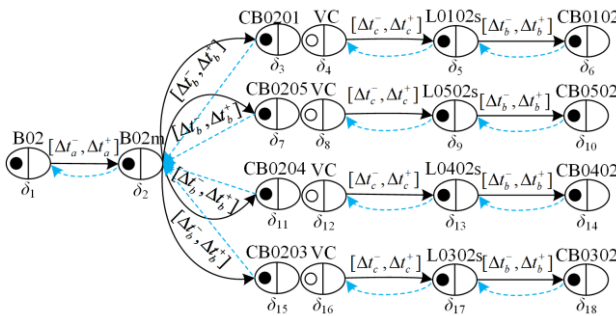Fig. A4. TTPS-based fault diagnosis model of L1011.

Fig. A5. TTPS-based fault diagnosis model of B02.
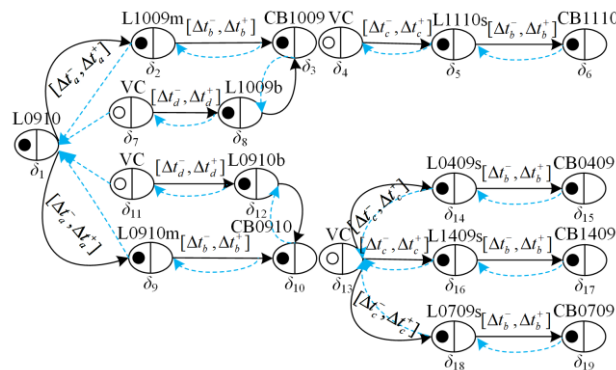

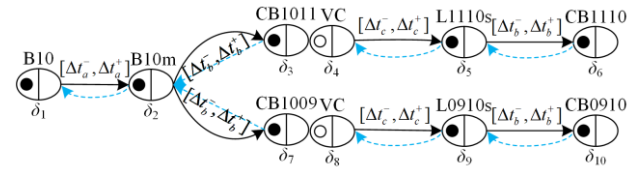Fig. A6. TTPS-based fault diagnosis model of L0910.

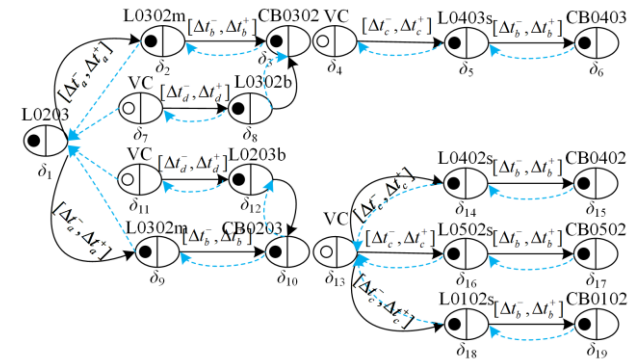Fig. A7. TTPS-based fault diagnosis model of B10.

Fig. A8. TTPS-based fault diagnosis model of L0203.

ACKNOWLEDGMENT

Not applicable.

AUTHORS' CONTRIBUTIONS

Kequan Zhou: write original draft, formal analysis and investigation. Tao Wang: write review & editing and supervision. Xiaotian Chen: data curation and investigation. Quanlin Leng: data curation. All authors read and approved the final manuscript.

FUNDING

AVAILABILITY OF DATA AND MATERIALS

Not applicable.

DECLARATIONS

Competing interests: The authors declare that they have no known competing financial interests or personal relationships that could have appeared to influence the work reported in this paper.

AUTHORS' INFORMATION

Kequan Zhou received the B.S. degrees in electrical engineering from Panzhihua University, Panzhihua, China, in 2020, and the M.S. degrees in electrical engineering from Xihua University, Chendu, China, in 2023. Currently, he is working in the Zigong Power

Supply Company of State Grid Sichuan Electric Power Company. His major research interests include fault diagnosis of power systems, and tissue like P systems.

Tao Wang received the Ph.D. degree in electrical engineering at the Southwest Jiaotong University, Chengdu, China, in 2016. She worked as a visit student in the Computer Science and Artificial Intelligence, University of Sevilla, Sevilla, Spain, during 11/2013 to 11/2014. She was a lecturer in Xihua University, China (2017-2019). She is currently an associate professor in the School of Electrical Engineering and Electronic Information at Xihua University since 2019. Her research interests include artificial intelligence and its application in electrical power systems.

Xiaotian Chen received the B.S. degrees in electrical engineering from Sichuan University of Science & Engineering, Yibin, China, in 2019, and the M.S. degrees in electrical engineering from Xihua University, Chengdu, China, in 2022. Currently, he is working in the Zizhong Power Supply Branch of State Grid Sichuan Electric Power Company. His major research interests include fault diagnosis of power systems, and spiking neural P systems.

Quanlin Leng received the B.S. degree in electrical engineering from Xihua University, Chengdu, China in 2022. He is currently enrolled in a M.S. degree in the Electrical Engineering in Xihua University. His major research interests include fault prediction and fault diagnosis of power systems.

REFERENCES

[1] T. Wang, X. G. Wei, and T. Huang *et al.*, "Modeling fault Propagation paths in power systems: a new framework based on event SNP systems with neurotransmitter concentration," *IEEE Access*, vol. 7, pp. 12978-12808, Dec. 2019.
[2] B. Ghosh, A. K. Chakraborty, and A. R. Bhowmik, "Reliability and efficiency enhancement of a radial distribution system through value-based auto-recloser placement and network remodelling," *Protection and Control of Modern Power Systems*, vol. 8, no. 1, pp. 1-14, Jan. 2023.
[3] D. Ma, Y. Liang, and X. Zhao *et al.*, "Multi-BP expert system for fault diagnosis of power system," *Engineering Applications of Artificial Intelligence*, vol. 26, no. 3, pp. 937-944, Mar. 2013.
[4] C. Yuan, Y. Liao, and L. Kong *et al.*, "Fault diagnosis method of distribution network based on time sequence hierarchical fuzzy petri nets," *Electric Power Systems Research*, vol. 191, Jan. 2021.
[5] Y. Zhang, Y. Zhang, and F. Wen *et al.*, "A fuzzy petri-net based approach for fault diagnosis in power systems considering temporal constraints," *International Journal of Electrical Power & Energy Systems*, vol. 78, pp. 215-224, Jun. 2016.
[6] X. Zhang, S. Yue and X. B. Zha, "Method of power grid fault diagnosis using intuitionistic fuzzy petri nets," *IET Generation Transmission & Distribution*, vol. 12, no. 2, pp. 295-302, Jun. 2018.
[7] Z. Jiang, Z. Li, and N. Wu *et al.*, "A petri net approach to fault diagnosis and restoration for power transmission systems to avoid the output interruption of substations," *IEEE Systems Journal*, vol. 12, no. 3, pp. 2566-2576, Sep. 2018.
[8] Y. Ge, X. Wang, and G. Zhu *et al.*, "Decentralized fault diagnosis of labeled Petri nets by basis markings," *Power System Protection and Control*, vol. 50, no. 15, pp. 178-185, Aug. 2022. (in Chinese)
[9] A. F. Novelo, E. Q. Cucarella, and E. G. Moreno *et al.*, "Fault diagnosis of electric transmission lines using modular neural networks," *IEEE Latin America Transactions*, vol. 14, no. 8, pp. 3663-3668, Aug. 2016.
[10] J. Chen, J. Gao, and Y. Jin *et al.*, "Fault diagnosis in distributed power-generation systems using wavelet based artificial neural network," *Protection and Control of Modern Power Systems*, vol. 23, no. 1, pp. 53-59, Feb. 2021.
[11] Z. Li, Z. Jiao, and A. He *et al.*, "A denoising-classification neural network for power transformer protection," *Protection and Control of Modern Power Systems*, vol. 7, no. 1, pp. 814-827, Dec. 2022.
[12] S. A. Siddiqui and Prashant, "Optimal location and sizing of conglomerate DG-FACTS using an artificial neural network and heuristic probability distribution methodology for modern power system operations," *Protection and Control of Modern Power Systems*, vol. 7, no. 1, pp. 124-148, Mar. 2022.
[13] B. Song, K. Li, and D. Orellana-Martın *et al.*, "A survey of nature-inspired computing," *ACM Computing Surveys*, vol. 54, no. 1, pp. 1-31, Jan. 2022.
[14] G. Păun, "A dozen of research topics in membrane computing," *Theoretical Computer Science*, vol. 736, pp. 76-78, Aug. 2018.
[15] B. Song, K. Li, and D. Orellana-Martın *et al.*, "Cell-like P systems with evolutional symport/antiport rules and membrane creation," *Information and Computation*, vol. 275, Dec. 2020.
[16] Y. Zhu, Y. Li, and B. Song *et al.*, "Time-free solution to independent set problem using P systems with active membranes," *Fundamenta Informaticae*, vol. 182, no. 3, pp. 243-255, Oct. 2021.
[17] F. G. C. Cabarle, X. Zeng, and N. Murphy *et al.*, "Neural-like P systems with plasmids," *Information and Computation*, vol. 281, Dec. 2021.
[18] T. Wang, W. Liu, and L. Valencia-Cabrerab *et al.*, "A novel fault diagnosis method of smart grids based on memory spiking neural P systems considering measurement tampering attacks," *Information Science*, vol. 596, pp. 520-536, Jun. 2022.
[19] T. Wu, L. Zhang, and Q. Lyu *et al.*, "Asynchronous spiking neural P systems with local synchronization of rules," *Information Science*, vol. 588, pp. 1-12, Apr. 2022.
[20] Y. Wang, T. Wang, and L. Liu *et al.*, "A fault segment location method for distribution networks based on spiking neural P systems and Bayesian estimation,"

Protection and Control of Modern Power Systems, vol. 8, no. 1, pp. 1-12, Jan. 2023.

[21] B. Song, Y. Hu, and H. N. Adorna *et al.*, "A quick survey of tissue-like P systems," *Romanian Journal of Information Science and Technology*, vol. 21, no. 3, pp. 310-321, 2018.

[22] B. Song, C. Zhang, and L. Pan, "Tissue-like P systems with evolutional symport/antiport rules," *Information Science*, vol. 378, pp. 177-193, Feb. 2017.

[23] L. Pan, A. Alhazov, and H. Su *et al.*, "Local synchronization on asynchronous tissue P systems with sym-port/antiport rules," *IEEE Transactions on Nanobioscience*, vol. 19, no. 2, pp. 315-320, Apr. 2020.

[24] D. Orellana-Martın, L. Valencia-Cabrerab and M. J. Perez-Jimenez, "P systems with evolutional communication and division rules," *Axioms*, vol. 19, no. 4, pp. 327, Dec. 2021.

[25] B. Song and L. Pan, "The computational power of tissue-like P systems with promoters," *Theoretical Computer Science*, vol. 641, no. 16, pp. 43-52, Aug. 2016.

[26] B. Song, X. Zeng, and M. Jiang *et al.*, "Monodirectional tissue P systems with promoters," *IEEE Transactions on Cybernetics*, vol. 51, no. 1, pp. 438-450, Jul. 2020.

[27] B. Song, K. Li and X. Zeng, "Monodirectional evolutional symport tissue P systems with promoters and cell division," *IEEE Transactions on Parallel and Distributed Systems*, vol. 33, no. 2, pp. 332-342, Mar. 2021.

[28] Y. Luo, Y. Zhao and C. Chen, "Homeostasis tissue-like P systems," *IEEE Transactions on Nanobioscience*, vol. 20, no. 1, pp. 126-136, Sep. 2020.

[29] Y. Luo, P. Guo, and Y. Jiang *et al.*, "Timed homeostasis tissue-like P systems with evolutional symport/antiport rules," *IEEE Access*, vol. 8, pp. 131414-131424, Jun. 2020.

[30] A. Păun and G. Păun, "The power of communication: P systems with symport/antiport," *New Generation Computing*, vol. 20, no. 3, pp. 295-305, Sep. 2002.

[31] R. Freund and M. Oswald, "Modelling grammar systems by tissue P systems working in the sequential mode," *Fundamenta Informaticae*, vol. 76, no. 3, pp. 305-323, Mar. 2007.

[32] R. Freund, G. Păun and M. J. Perez-Jimenez, "Tissue P systems with channel states," *Theoretical Computer Science*, vol. 330, no. 1, pp. 101-116, Jan. 2005.

[33] X. Tian and X. Liu, "Improved hybrid heuristic algorithm inspired by tissue-like membrane system to solve job shop scheduling problem," *Processes*, vol. 9, no. 2, pp. 1-18, Jan. 2021.

[34] A. H. Christinal, D. Dıaz-Pernil, and P. Real, "Region-based segmentation of 2D and 3D images with tissue-like P systems," *Pattern Recognition Letters*, vol. 32, no. 16, pp. 2206-2212, Dec. 2011.

[35] J. Xue, S. Yan, and Y. Wang *et al.*, "Unsupervised seg-mentation of choroidal neovascularization for optical coherence tomography angiography by grid tissue-like membrane systems," *IEEE Access*, vol. 7, pp. 143058-143066, Sep. 2019.

[36] H. Peng, J. Wang, and P. Shi *et al.*, "Fault diagnosis of power systems using fuzzy tissue-like P systems," *Integrated Computer-Aided Engineering*, vol. 24, no. 3, pp. 1-11, Sep. 2017.

[37] T. Kang, W. Wu, and B. Zhang *et al.*, "Temporal abductive reasoning based diagnosis and alarm for power grid," *Proceedings of the CSEE*, vol. 30, no. 19, pp. 84-90, Jul. 2010. (in Chinese)

[38] W. Guo, F. Wen, and G. Ledwich *et al.*, "A new analytic approach for power system fault diagnosis employing the temporal information of alarm messages," *Journal of Electrical Power & Energy Systems*, vol. 43, no. 1, pp. 1204-1212, Dec. 2012.

[39] Y. Zhang, Y. Zhang, and F. Wen *et al.*, "Power system fault diagnosis with an enhanced fuzzy petri accommodating temporal constraints," *Automation of Electric Power Systems*, vol. 38, no. 5, pp. 66-72, Mar. 2014. (in Chinese)

[40] B. Xu, X. Yin, and X. Yin *et al.*, "Fault diagnosis of power systems based on temporal constrained fuzzy Petri nets," *IEEE Access*, vol. 7, pp. 101895-101904, Jul. 2019.

[41] J. Yang, Z. He, and T. Zhang, "Power system fault-diagnosis method based on directional weighted fuzzy petri nets," *Proceedings of the CSEE*, vol. 30, no. 34, pp. 42-49, Dec. 2010. (in Chinese)

[42] G. Xiong, D. Shi, and L. Zhu *et al.*, "A new approach to fault diagnosis of power systems using fuzzy reasoning spiking neural P systems," *Mathematical Problems in Engineering*, vol. 2013, 2013.

[43] W. Chen, "Online fault diagnosis for power transmission networks using fuzzy digraph models," *IEEE Transactions on Power Delivery*, vol. 27, no. 2, pp. 688-698, Apr. 2012.

[44] T. Bi, L. Jiao, and Z. Yan *et al.*, "Graph partitioning method for distributed fault section estimation system in power network-s," *Automation of Electric Power Systems*, vol. 25, no. 16, pp. 16-21, Aug. 2001. (in Chinese)

[44] G. Yang, F. Ji, and X. Liu *et al.*, "Fault location of a distribution network hierarchical model with a distribution generator based on IBES," *Power System Protection and Control*, vol. 50, no. 18, pp. 1-9, Sep. 2022. (in Chinese)